Preparation of Coal-Kaolinite Nano Composites and Investigation of Their Use to Remove Methyl Orange from Water

Misael Silas Nadiye-Tabbiruka[*], **Fortunate Phenyo Sejie**

Department of Chemistry, University of Botswana, Gaborone

Abstract   Coal/clay nano composites of ratios 1:1, 1:4, 4:1 were successfully prepared and characterised by electron microscopy. They were then used to study kinetics and thermodynamics of removal from water of methyl orange of various concentrations, various pH and at various temperatures. The coal:clay ratios 1:1 and 4:1 performed equally but better than 1:4 and the individual coal and clay samples. The swelling in coal and in clay which occurs on initial adsorption appears to have been eliminated by the miniaturisation. The adsorption capacity of the composites was found to be higher than that of either the clay or the coal on their own but it is still lower than that of commercial activated carbon.

Keywords   Adsorption, Nano composite, Adsorption kinetics, Adsorption thermodynamics, Coal, Kaolinite

1. Introduction

Nano particles, colloid materials with average size range of 1-100nm, are very useful for fundamental and diversified applications [1]. They are used in several industrial applications including optical sensor devices, thermal conducting gel, body repairing, cancer therapy, high performance batteries, chromatography columns and magnetic fluids to mention but a few. In pure form they cannot be used because of their tendency to agglomerate. To avoid these problems, nano particles are embedded on a support material to form nano composites instead [2]. Preparation methods for nano composite particles depend on their intended use. Two most widely used methods for preparing nanoparticle/composite are chemical and physical procedures [3]. Chemical synthesis involves the use of chemicals reactions to produce nano units while physical methods involve breaking down of large material by mechanical grinding until the particles are in the nano range [4]. Furthermore, coal and Clay minerals are widely used in several industries and fields such as in polymers nano-composites adsorbents fields, in heavy metal ion adsorption, ceramics, and paper fillings [5-7] as well as in nano composites designed for specific applications. These include anion adsorbents [8,9], cation adsorbents [10,11,8]

and in some cases adsorbents to aid purification of water by removing multiple contaminants simultaneously [12].

In this paper we present the preparation and characterisation of coal/clay nano composites. These composites are then used to investigate their possible use to purify water. This is done by studying the adsorption kinetics and thermodynamics of removal from water of methyl orange, an organic pollutant.

1.1. Adsorption Kinetics

1.1.1. Lagergren Pseudo 1st Order Kinetics'Model

Lagergren pseudo first-order rate equation, the earliest known model describing the adsorption rate based on the adsorption capacity [9], is given below (equation 1):

$$\log(q_e - q_t) = log q_e - \frac{k_1}{2.303}t \qquad (1)$$

Where k_1 is the pseudo first order rate constant in g/mg* min, q_e is the amount adsorbed at equilibrium, q_t is the amount adsorbed at any time t, in minutes. If the data obtained fits the model, a plot of $\log((q_e - q_t))$ against t should give a straight line and k_1 can be determined from the slope and q_e from the intercept. The rate constant the theoretical and the equilibrium amount adsorbed q_e can be derived from this model plot.

1.1.2. The Lagergren Pseudo Second Order Model is Given by Equation 2

$$\frac{dq_t}{d_t} = k_2(q_e - q_t)^2 \qquad (2)$$

once again a plot of t/q_t against t should be linear and the second order rate constant k_2 can be determined from the

* Corresponding author:
nadiyemst@yahoo.com (Misael Silas Nadiye-Tabbiruka)

intercept and q_e from the slope)

1.2. Adsorption Thermodynamics

Adsorption thermodynamics' data is analysed using Langmuir, Freundlich and Temkin models, in this work the data did not fit the Langmuir isotherm hence it was not used.

The Freundlich adsorption model is given by equation 3 and 4

$$q_e = K_f\, Ce^{1/n} \qquad (3)$$

which linearizes to

$$\ln q_e = \ln K_f + (1/n)\ln C_e, \qquad (4)$$

a linear plot of $\ln q_e$ against $\ln C_e$ will give the constant K_f from the intercept and the constant n from the slope.

Temkin adsorption model is given by equation 5

$$q_e = B \ln A + B \ln C_e, \qquad (5)$$

and from a linear plot of the quantity adsorbed q_e against $\ln C_e$ the constants A (Temkin equilibrium binding constant) and B (a constant related to heat of adsorption in J/mol) can be determined from the slope and the intercept. In this case $B = RT/b_T$ where b_T is Temkin isotherm constant.

A consideration of adsorption equilibrium results in equation 6 below;

$$K_0 = \frac{V_s q_e}{V_e C_e} \qquad (6)$$

Where K_o is the thermodynamic equilibrium constant q_e is the surface concentration of dye on adsorbent (mol g^{-1}) C_e is the concentration of dye in the equilibrium solution (mol L^{-1}), V_s is the activity coefficient of the adsorbed dye and V_e is the activity coefficient of dye in solution

For very dilute solutions $K_0 = \frac{q_e}{c_e}$ hence the values of K_o is obtained from a plot of $\ln {q_e}/{c_e}$ versus q_e. An extrapolation of q_e to zero [13] gives an intercept equal to $\ln K_o$.

Thus the thermodynamics parameters can be calculated from equation 7 and 8 given below.

$$\Delta G^\circ = -RT \ln K_0 \qquad (7)$$

$$\ln K_o = \frac{\Delta S^\circ}{R} - \frac{\Delta H^\circ}{RT} \qquad (8)$$

2. Experimental

2.1. Materials

2.1.1. Adsorbent

The coal-clay nano-composites were prepared using a method adopted from the literature [14,15] in which nano-composites with activated interfaces were prepared by mechanical grinding of magnesium hydrides used for storing hydrogen.

Mixtures of 1:1, 1:4 and 4:1 mass ratio of the coal (ESEM fig 1a) to clay (ESEM fig 1b [16]) were made and used to prepare the composites. The resulting powder was then soaked in deionised water at room temperature under ultrasonic stirring, to form a homogeneous mixture. The resulting mixture was subjected to mechanical grinding until the slurry mixture was formed in water [17]. The resulting mixture was centrifuged at 2000 rpm. Water was decanted and the top fine particles were dried in an oven. The resulting product was analysed with an Environmental Scanning Electron Microscope (ESEM figure 1c). This was repeated until particle reduction to nano level was achieved. These were used to investigate adsorption experiments.
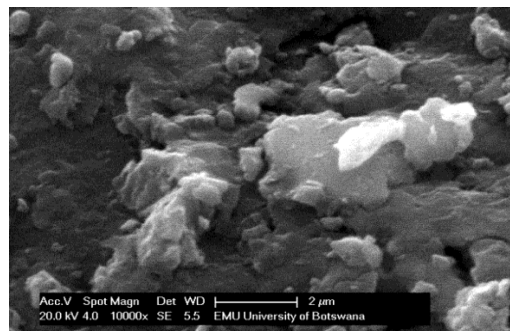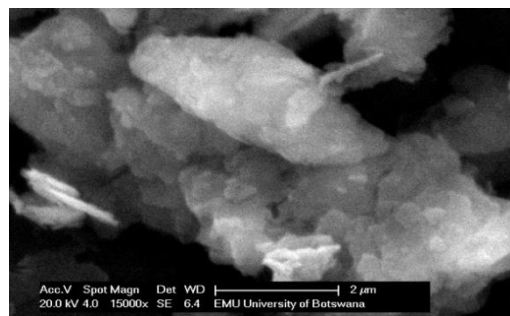

Figure 1a.   ESEM microgra of Morupule coal

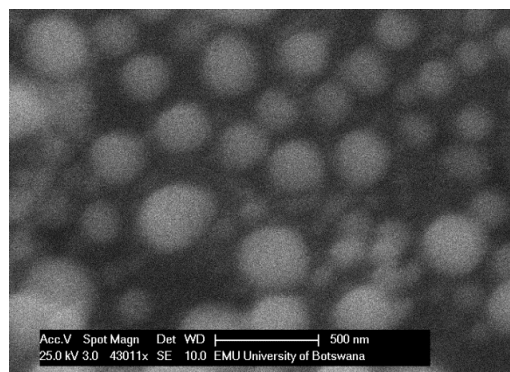**Figure 1b.**   ESEM microgram of Lobatse clay [16]

Figure 1c.   SEM microgram of a 1:1 clay: coal composites

2.1.2. Adsorbate Methyl Orange (MO)

Methyl orange (Anionic, water soluble azo dye) powder ($C_{14}H_{14}N_3NaO_3S$, figure 2a) supplied by SAARCHEM, South Africa was used without any further purification. A solution of the dye was made by dissolving a known weight into double distilled de-ionised water. Other required dye concentrations were prepared by serial dilution. Several of these concentrations were used to obtain a calibration curve

of absorbance against concentration at a predetermined wavelength of maximum absorption λ=463 nm using a UV-Visible spectrophotometer spectronic 20. Concentrations of unknown samples were then determined from the calibration curve.
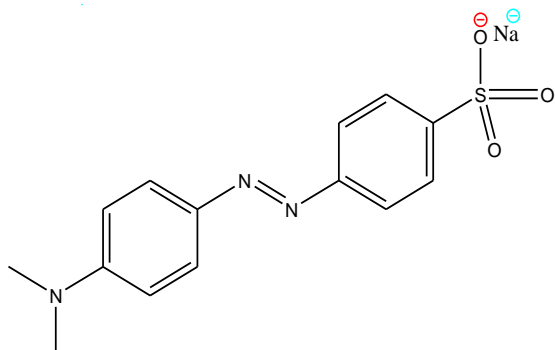

Figure 2. Methyl orange structure

2.2. Procedure

2.2.1. Studies of Adsorption Kinetics

0.05g of the nanocomposite was added to 20 ml of MO solution in a screw capped bottle contained in a water bath at constant temperature, and a stop clock was simultaneously started. Samples of the supernatant liquid were drawn off after predetermined time intervals, centrifuged at 2000 revolutions per minute for a minute or so to assist the separation of the nano particles from the supernatant, filtered using an appropriate filter paper and then their absorbance were taken using a UV/VIS spectrophotometer at a wavelength of 463 nm. The amount adsorbed was obtained by difference between the initial concentrations and the concentrations at the sampling time and plotted against time. The experiment was repeated for various MO concentrations, reaction temperature and pH.

2.2.2. Studies of Adsorption Thermodynamics

In this section, a batch technique was used. The clay-coal composite (0.05 g) was added to each of several 250 mL screw capped bottles containing 200ml of methyl orange of different initial concentrations. The bottles were kept in a thermostatic water bath shaker at a speed of 220 rpm for 4 hours at constant temperature. After the samples had reached equilibrium, the Solutions were centrifuged, filtered using 0.45 μm filter paper and the equilibrium concentrations of the filtrates were determined spectrophotometrically as before. The amount adsorbed at equilibrium, q_e (mol/g), was calculated by using equation 9 below:

$$q_{e=}\left[\frac{(C_0-C_t)}{m}\right] * V \qquad (9)$$

Where C_o is the initial concentration of the dye and C_t is the concentration of the dye after time t (minutes) (mol/L), V (L) is the volume of methyl orange solution and m(g) is the weight of coal- clay composite. The equilibrium adsorption q_e values were used to plot an adsorption isotherm.

3. Results and Discussion

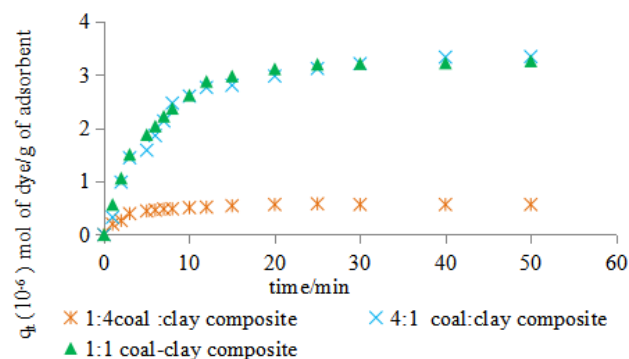### 3.1. Analysis of Results from Adsorption Kinetics Studies

Figure 3a. Adsorption of methyl orange dye 3.14×10^{-5} M on to the composites at pH 7.18 and 300K

Figure 3a presents the adsorption kinetics of the dye onto the composites at 300K. For the three composites, the process reaches equilibrium within 30minutes. The composites show different adsorption capacities and different rates of adsorption at the various ratios. The nano composite with the highest coal content removes more of the dye compared to the other two. The nano composite with highest mass of coal and that with equivalent masses of coal and clay show the highest adsorption capacity and rate. The nano composite with the lowest coal content shows lowest adsorption capacity.
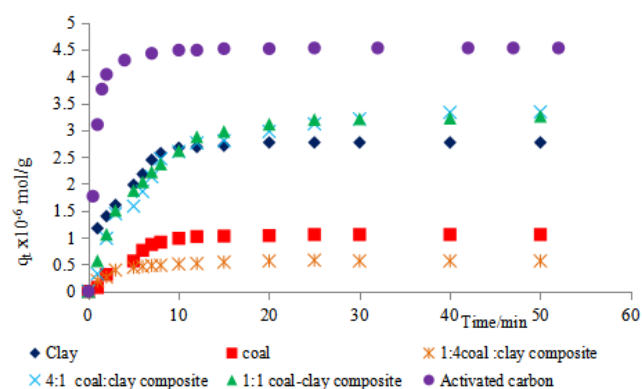

Figure 3b. Studies of methyl orange 3.14×10^{-5} M adsorption onto various adsorbents at 300K

Figure 3b compares all the adsorbents studied in this work with commercial activated carbon. It is clear that the commercial adsorbent is still outperforming our prepared samples. However, the nano composites and acid activated clay are closest to the commercial activated carbon samples.

3.1.1. Testing data on Kinetic Models

The chi (χ^2) test was used to test the closeness of the calculated/theoretical data to the experimental data, by using equation 10.

$$\chi^2 = \sum\left(\frac{[q_{e\,exp}-q_{e\,theo}]^2}{q_{e\,theo}}\right) \qquad (10)$$

where

$q_{e\,exp}$ is the experimentally determined equilibrium amount adsorbed

$q_{e\,theo}$ is the theoretical equilibrium amount adsorbed determined from the kinetics' model equations

From this equation a small value of χ^2 shows the model test fits the experimental data well.

Adsorption of methyl orange onto Morupule coal:Lobatse clay nano composite was investigated by fitting the raw data to the lagergren pseudo first and pseudo second order kinetic models and the resulting plots are given below (see fig 4, table 1).
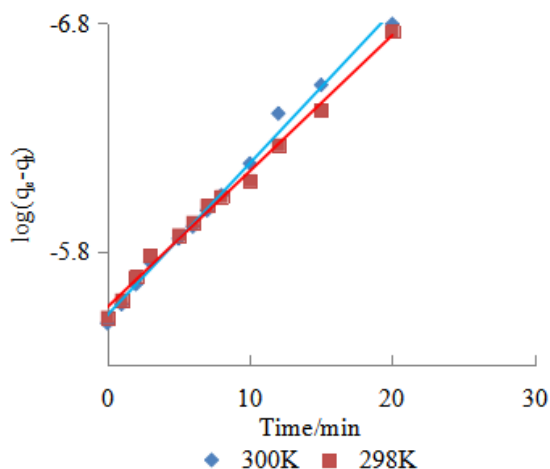

Figure 4. Lagergren pseudo first order model plot for the adsorption of methyl orange onto the 1:1 composite at T= (298 and 300) K, 5.49×10^{-5} M, pH 7.18 and 10 g/L sorbent dosage
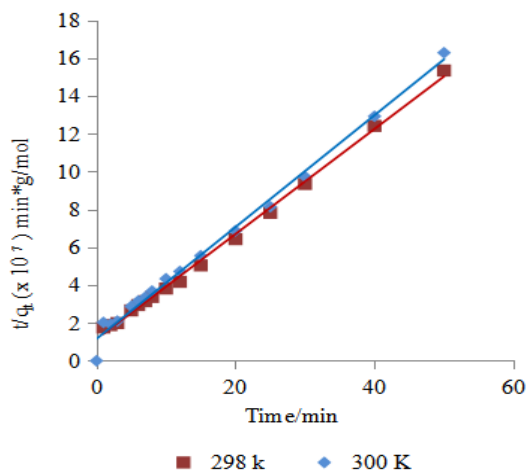

Figure 5. Lagergren pseudo second order kinetics model for the adsorption of methyl orange onto the 1:1 coal: clay composite at T= (298 and 305) K, 5.49×10^{-5} M, pH 7.18 and 10 g/L sorbent dosage

Table 1. Lagergren pseudo first order parameters

Temp	lgk	Exper q_e E-7	Theor q_e E-7	R^2
298	-0.1531	32.7160	32.716	0.9924
300	-0.1370	30.8337	30.834	0.9932
χ^2		1.052×10^{-10}		

The sorption process was investigated by fitting the raw data onto the Lagergren pseudo first and second order kinetics models. The sorption process fitted the Lagergren pseudo second order kinetics model (fig (5) slightly better than the pseudo first order (see fig 4) confirming the continuation of simultaneous occurrence of two mechanisms or one mechanism in two different environment thought to be inner and outer surfaces, even on the nano composite. One would expect miniaturisation to eliminate delayed adsorption onto internal area originating from swelling. The results should hence fit the Lagergren pseudo first order model better for the nano-composite. This was not very clear as the results fitted both models. However, the fitting onto the pseudo second order was slightly better. This could be because of the clustering of the nano particles which creates temporary slit like pores out of spaces between particles. The sorption process was faster on the nano-composite than on the other two adsorbents (coal and clay fig 3b) as would be expected due to miniaturisation to eliminate or reduce internal areas.

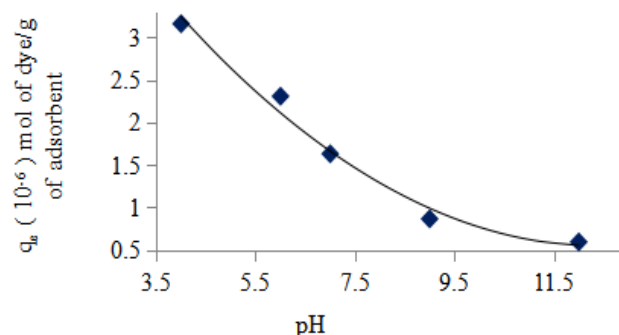### 3.2. Thermodynamics' Data Analysis

Figure 6. Effect of pH change on the equilibrium adsorption of methyl orange onto the 1:1 composite at 3.14×10^{-5} M, 298 K and 10 g/L sorbent dosage

Figure 6 shows a decrease in the adsorption capacity of the nano composites with an increase in pH indicating that adsorption is more favoured in acid conditions than in basic conditions.

As pH is increased to more basic conditions, the double bond conjugation is lost and a proton is lost, and the MO molecule rearranges to form a negatively charged species (figure 7a). The positive charges have been neutralized. Due to excess anions in the solution, there will be repulsion of the dye by the negatively charged surfaces of the adsorbents, also an increase in pH leads to the modification of the pi (Π) system delocalization pattern.

In the literature, the uptake of methyl orange on several adsorbents was similarly found to be favoured at lower pH (acidic medium) [18]. Furthermore, at lower pH, the surface of the adsorbent was found to be activated by the acid in solution and the dye became protonated (see fig 7b, c &d) thus enhancing the adsorption process [9].
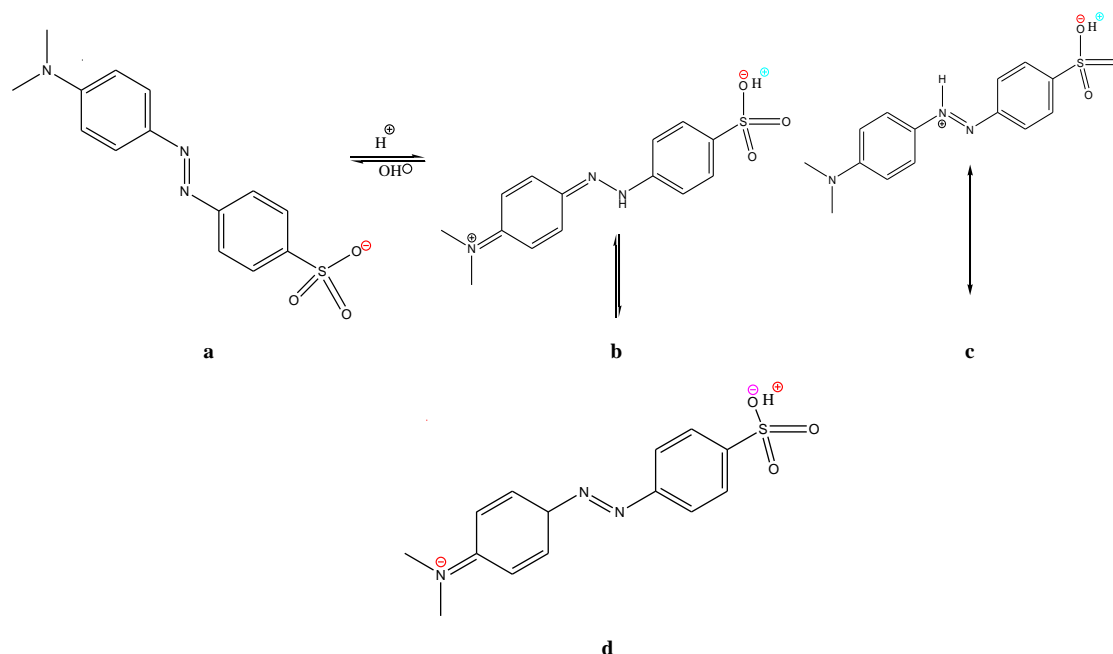
3.2.1. Effect of pH on the Structure of the Dye

Figure 7. Alkaline form of Methyl orange (a) and its mono-protonated zwitter ionic structures under acidic conditions(b, c and d)
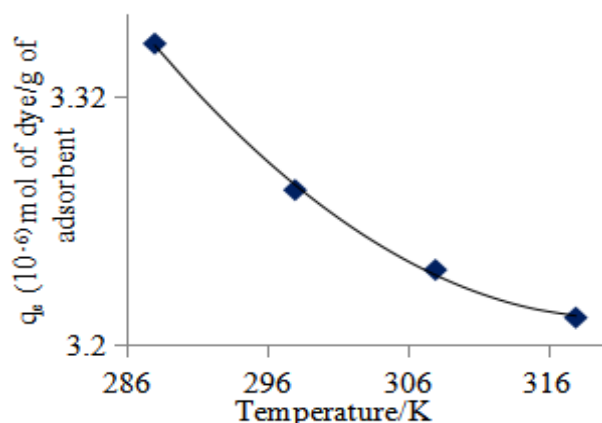
3.2.2. Temperature Effect

Figure 8. Effect of change in temperature on the equilibrium adsorption of methyl orange onto the 1:1 composite at 3.14×10^{-5} M, 10 g/L sorbent dosage and pH 7
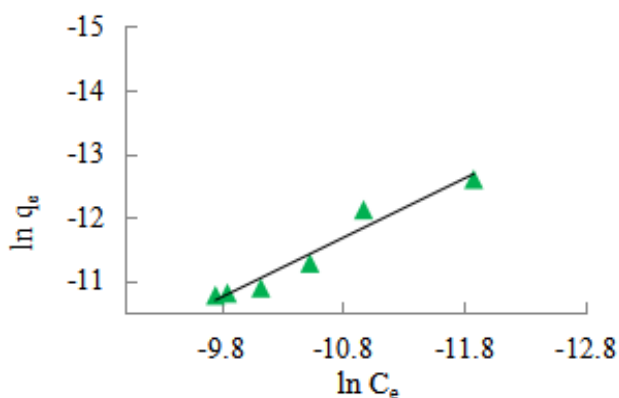

Figure 9. Freundlich isotherm for the adsorption of methyl orange onto 1:1 nano composite at 298 K, pH 7.18 and 10 g/L sorbent dosage
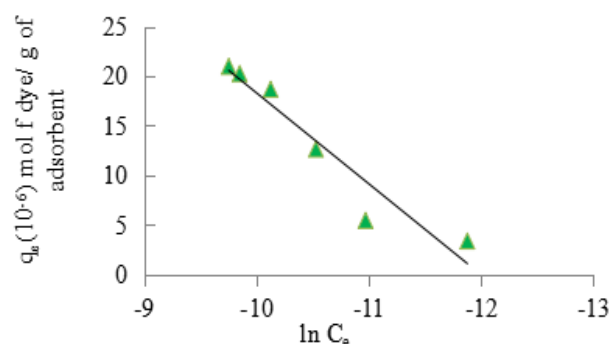

Figure 10. Temkin isotherm for the adsorption of methyl orange onto the 1:1 coal-clay composite at 298 K, pH 7.18 and 10 g/L sorbent dosage

Table 2

Isotherm model	Composite parameter	Parameter magnitude
Freundlich	K_f (mol/{g/L}$^{1/n}$)E-02	0.2078
	$\frac{1}{n}$ (g/L)	0.9355
	R^2	0.9553
Temkin	K_t/A_t (L/g) E05	1.6418
	b E-6 j/mol	9.1600
	R^2	0.9181

Studies of the thermodynamics of adsorption of methyl orange onto nano-composites by the batch technique were conducted and the data obtained was analysed using various thermodynamic models outlined earlier. The effects of solution pH and solution temperature were investigated. An decrease in temperature of the dye solution increased the capacity of the adsorbents (see fig 8) indicating a physisorption process. This is further confirmed by the low entropies and heats of adsorption obtained (see table 3).

The process onto the 1:1 composite is favoured by lower pH (see fig 6). This is probably due to the resultant net positive charge on the dye molecule at lower pH (see fig 7) which weakly interacts with the negatively charged adsorbent surface.
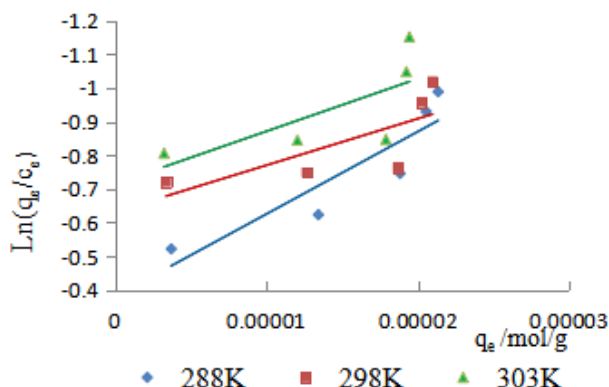

Figure 11.   Plot for the determination of K_o at various temperatures for the adsorption of methyl orange onto the 1:1 composite
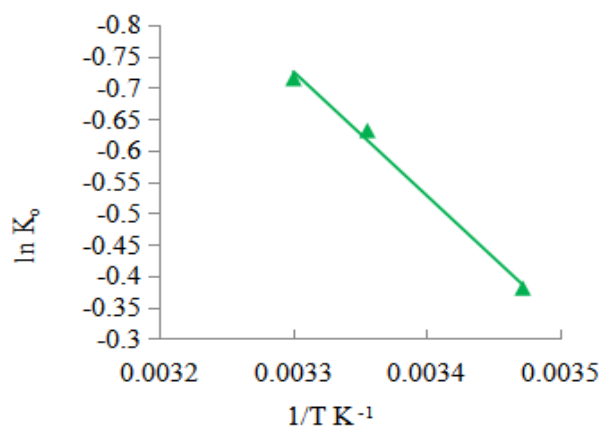

Figure 12.   Vant'Hoff plot for the adsorption of methyl orange onto the 1:1 nano composite

Table 3.   Thermodynamic properties for the adsorption of MO on 1:1 nano composite

T/K	R^2	$\Delta G°$ (kJ/mol)	$\Delta H°$ (kJ/mol)	$\Delta S°$ (kJ/mol)
288	0.817	0.9120		
298	0.558	1.5655	-16.421	0.060227
303	0.507	1.8008		

The adsorption capacity of the clay, the 1:1 and 4:1 composite adsorbents compared reasonably well with that of activated carbon in spite of the much larger surface area of over 500 m^2g^{-1} for the commercial activated carbon (see fig 3b). The trend of the capacity was found to be: Activated carbon > 4:1 coal: clay composite ~ 1:1 coal: clay composite > 1:4 coal: clay composite. The changes in adsorption capacity in the nano composites appear to indicate the presence of some form of interaction in solid phase between the clay and coal nano-particles.

The Freundlich and Temkin isotherms models were found

to describe the sorbent-sorbate interaction for this study best (see figs 9&10). The heats of adsorption were small and inconclusive in this case as for the coal and clay [17]. The data from adsorption onto the surface of the nano-composite fitted the Freundlich model better confirming that it was heterogeneous just like the coal and the clay. This correlated well with the scanning electron microscope micrograms; which showed varying sizes of nano agglomerates and irregular surfaces for coal and clay particles [19] (see fig 1a, 1b and 1c).

4. Conclusions

The possible use of the composites as water purifiers investigated by studying their interaction thermodynamics and kinetics at various temperatures and solution pH found that adsorption capacity, q_e, increases with increasing initial concentration (see fig 9), decreases with increasing pH (see fig 6) and decreases with increasing temperature (see fig 8). The enthalpies and entropies of adsorption were found to be -16.421 $kJmol^{-1}$ and 0.060 $kJmol^{-1}$ respectively (see table 3) for the 1:1 composite indicating that physisorption is still the mechanism in operation.

It is evident that miniaturisation to nano level greatly improves their capacity and rate for adsorbing methyl orange compared to that of the individual clay or coal samples. The fitting of the kinetics data on Lagergren pseudo second order was better than that on the pseudo first order. However the fitting on pseudo first order greatly improved from the cases of the individual coal and clay adsorbents observed in earlier work [21]. This indicates that as a result of miniaturisation, the internal areas originally accessed after swelling caused by initial adsorption which often lead to a second adsorption surge was now easily available at the start. There was therefore no adsorption initiated expansion of the material which was observed for both the clay and the coal individually [21,22]. However, its contribution to the overall available area is less that the contribution from steam activation since the commercial steam activated carbon still performed better indicating that steam activation is more effective in creating a super adsorbent than miniaturisation. This is therefore a cheap viable method of removing methyl orange comparable to many others [23-26].

REFERENCES

[1]   Kholoud M.M. Abou El-Nour Ala'a Eftaiha, Abdulrhman Al-Warthan *Synthesis and applications of silver nanoparticles* Arabian Journal of Chemistry. - (2010). - Vol. 3. - pp. 135–140; Danielle Thandi Sass, Emile Salomon Massima Mouele and Natasha Ross *Nano Silver-Iron-Reduced Graphene Oxide Modified Titanium Dioxide Photocatalytic Remediation System for Organic Dye* (2019) DOI 10.3390/environments6090106.

[2] Mansor Bin Ahmad Kamyar Shameli, Majid Darroudi, *Synthesis and Characterization of Silver/Clay Nanocomposites by chemical reduction method* [Journal] // American Journal of Applied Sciences . (2009). : Vol. 6 . - pp. 1909-1914.

[3] Olfat M. Sadek Safenaz M. Reda, Reem K. Al-Bilali *Preparation and Characterization of Silica and Clay-Silica Core-Shell Nanoparticles Using Sol-Gel Method* [Journal] // Advances in Nanoparticles. - (2013). - Vol. 2. - pp. 165-175.

[4] Moncada E, Quijada, R, and Zapata, P, *Modification of Clays by Sol-Gel Reaction and their use in the Ethylene in situ polymerration for obtaining Nano particles* [Journal] // Journal of Nanomaterials. -(2012): Vol. 1155. - pp. 1-7.

[5] Saeed, T.A., R.Muyeed, A. A.Sun, G., *Treatment of tannery wastewater in a pilot-scale hybrid constructed wetland system in Bangladesh.* Chemosphere, (2012). 88(9): p. 1065-73; Dina, A.; Scholz, Y.M. *Treatment of synthetic textile wastewater containing dye mixtures with microcosms.* Env. Sci. Poll. Res. Int. (2018), 25, 1980–1997.

[6] Bouaziz, I.C., C.Abdelhedi, R.Savall, A.Groenen Serrano, K., *Treatment of dilute methylene blue-containing wastewater by coupling sawdust adsorption and electrochemical regeneration.* Environ Sci Pollut Res Int, (2014).

[7] Attallah, M.F., I.M. Ahmed, and M.M. Hamed, *Treatment of industrial wastewater containing Congo Red and Naphthol Green B using low-cost adsorbent.* Environ Sci Pollut Res Int, (2013). 20(2): p. 1106-16.

[8] Kouotou Daouda, Abdoul Ntieche Rahman, Hambate Gomdje Valery, Ndi Julius Nsami, Abdoul Wahabou and Ketcha Joseph Mbadcam, *Adsorption equilibrium of nitrate ions onto oil palm shellsbased activated carbons*, Global journal of science frontier research: B chemistry (2018) 18(1) 36-52.

[9] Kiesel, I.P., M.Nase, J.Tiemeyer, S.Sternemann, C. Ruster, K.Wirkert, F. J.Mende, K.Buning, T.Tolan, M., *Temperature-driven adsorption and desorption of proteins at solid-liquid interfaces.* Langmuir, (2014). 30(8): p. 2077-2083.

[10] Dada A.O., Olalekan A.P., Olatunya A.M. and Dada O., *Langmuir, Freundlich, Temkin and Dubinin-Radushkevich isotherm studies of equilibrium sorption of Zn2+ onto phosphoric acid modified rice husks*, Journal of applied chemistry (2012) 3(1) 38-45.

[11] Asuha, S., X.G. Zhou, and S. Zhao, *Adsorption of methyl orange and Cr(VI) on mesoporous TiO2 prepared by hydrothermal method.* J Hazard Mater, (2010). 181(1-3): p. 204-210.

[12] Sven Herrmann, Laura De Matteis, Jesus M de la Fuente, Scott G Mitchell, and Carsten Streb *Removal of multi contaminants from water by Polyoxometalate supported ionic liquid Phases (POM-SILPs)*, Angew. Chem. Int. Ed. (2017) 56 1667-1670.

[13] Hardijeet K. Boparai, M.J., Denis M.O'Carroll, *Kinetics and thermodynamics of Cadmium ion removal by adsorption onto nano zerovalent iron particles.* Journal of Hazardous materials, (2010). 2010.11.029, 8.: p. 8.

[14] Robert Schulz, G.L., Guy Lalande, Jacques Huot, Sabin Boily, André Van Neste, *Nanocomposites with activated interfaces prepared by mechanical grinding of magnesium hydrides and use for storing hydrogen,* (2007). Patent number: 7201789.

[15] Arvind Kumar, Hara Mohan Jena; *Preparation and characterisation of high surface area activated carbon from Fox nut shell by chemical activation with H$_3$PO$_4$,* Results in Physics (2016) 651-658; Nady A. Fathy, Sohair A. Sayed Ahmad and Reham M. M. Abo el -enin, *Effect of activation temperature on textural and adsorptive properties of activated carbon derived from local reed biomass: Removal of p-nitrophenol,* Environmental research Engineering and management (2012), 1(59) 10 – 12.

[16] Zbik, M.S., R.S. Smart, and G.E. Morris, *Kaolinite flocculation structure.* J Colloid Interface Sci, (2008). 328(1): p. 73-80.

[17] Hato, Z., E. Mako, and T. Kristof, *Water-mediated potassium acetate intercalation in kaolinite as revealed by molecular simulation.* J Mol Model, (2014). 20(3): p. 2140; M.M.S. Ali, N. El-SAI, B.S. GIRGIS, *Evaluation and modelling of high surface area activated carbon from date frond and applications on some pollutants,* International journal of computationa Engineering Research (2014) 4(1) 70-78.

[18] Egwuonwu, P., *Adsorption methyl red and Methyl orange using different bark powder.* Academic research international (2013). 4(1): p. 330-338.

[19] B.H Hameed, D.K.M., A.L. Ahmad, *Equilibrium modeling and kinetic studies on the adsorption of basic dye by a low cost adsorbent: Coconut (Cos nucifera) bunch waste.* Journal of hazadous materials, (2008). 158: p. 65-72.

[20] A. Gurses, C.D., M. Yalcin, M. Acikyildiz, R. Bayrak, S.Karaca, *The adsorption of cationic dye, methylene blue on to clay.* Journal of hazadous materials, (2005). B131: p. 217-228.

[21] Sejie P. F. and Nadiye-Tabbiruka M.S. (2016) "*Removal of methyl orange (MO) from water by adsorption onto modified local clay*" Physical Chemistry 6(2) 39-48; Bessegato, G.G.; Cardoso, J.C.; Zanoni, M.V.B. Catal. Enhanced *photoelectrocatalytic degradation of an acid dye with boron-doped TiO2 nanotube anodes.* Today (2015), 240, 100.

[22] Nadiye-Tabbiruka M.S. and Sejie P.F., Coetze S.H. and Salamula E.J. (2015) "*A study of the adsorption of dyes from aqueous solution by Morupule coal*" Journal of advances in chemistry 11(9) 3959-3972.

[23] Lu, L.; Huiyao, Wang.; Wenbin, J.; Ahmed, Radhi,; M.; Pei, Xu. Comparison study on photocatalytic oxidation of pharmaceuticals by TiO2-Fe and TiO2-reduced graphene oxide nanocomposites immobilized on optical fibers. J. Haz. Mat. (2017), 333, 162–168.

[24] Milenova, K.; Zaharieva, K.; Stambolova, I.; Blaskov, V.; Eliyas, A.; Dimitrov, L. Photocatalytic performance of tio2, ceo2, zno and tio2-ceo2-zno in the course of methyl orange dye degradation. J. Chem. Tech. Met. (2017), 52, 13–19.

[25] José, O.; Carlos, M.N.R.; Carlos, H.F.; de Renê, S.C.; da Pablo, S.A. Rocha. Synthesis, Characterization and Enhanced Photocatalytic Activity of Iron Oxide/Carbon Nanotube/Ag-doped TiO2 Nanocomposites. J. Braz. Chem. Soc. 2(017), 28, 1678-4790.

[26] Reza, K.; Kurny, A.; Gulshan, F. Parameters affecting the photocatalytic degradation of dyes using TiO2: A review. Appl. Water Sci. 2(017), 7, 1569–1578.